Optics Communications 332 (2014) 301–310

Contents lists available at ScienceDirect

Optics Communications

journal homepage: www.elsevier.com/locate/optcom

Imaging properties of different types of microscopes in combination with an image inversion interferometer

Daniel Weigel *, Holger Babovsky, Armin Kiessling, Richard Kowarschik

Institute of Applied Optics, Abbe Center of Photonics, Friedrich Schiller University, Froebelstieg 1, Jena 07743, Germany

ARTICLE INFO

Article history:
Received 11 April 2014
Received in revised form
16 June 2014
Accepted 9 July 2014
Available online 19 July 2014

Keywords:
Image detection systems
Microscopy
Confocal microscopy
Interference microscopy
Scanning microscopy
Resolution

ABSTRACT

Image inversion microscopy enables an increase of the lateral resolution of optical microscopes. A huge advantage of the method is the possibility to combine it with different illumination techniques, because the required image inversion interferometer has to be added behind the microscope objective.

In this work, we investigate the influence of a pinhole on the resolution, the sectioning capability and the noise characteristics of a confocal fluorescence microscope combined with such an interferometer. Additionally, we demonstrate the benefits of image inversion interferometers for two-photon microscopes, as well as for extended-focus microscopes. As a result, the increase in information for interferometrically enhanced systems can be up to 500% in terms of the optical transfer function.

1. Introduction

In 2006 Sandeau et al. suggested an interferometric method to almost double the lateral resolution of a 4Pi-microscope by using image inversion optics [1,2]. The method makes use of the spatial incoherence of the fluorescent object to modify the observation-side point spread function (PSF). Later, this approach has been transferred to confocal fluorescence microscopes by Wicker and Heintzmann [3]. A huge advantage is the versatility of this technique. The necessary components have to be put behind the microscope objective, which enables the combination with different illumination methods such as confocal, two-photon or 4Pi. Hence, existing systems could be upgraded easily. Additionally, there have been suggestions to modify the illumination-sided PSF by image inversion interferometry [4].

In the first experimental realizations of image inversion microscopy, an improved resolution of up to 26% could be measured [5,7–9]. Furthermore, the records showed significantly improved contrasts. By using digital holography, it is also possible to apply this technique to coherent illuminating systems. Another advantage of this combination is the possibility to shift the image inversion and the scanning process completely to the digital post-processing [9].

It is already known that the choice of the pinhole size in front of the detectors of a confocal fluorescence microscope (CFM) combined with an image inverting interferometer is highly important for the lateral and axial dimension of the detection PSF [7,10]. For example, considering the case of an infinitesimal pinhole, the interferometrical illumination PSF is the same as the PSF of a conventional CFM. By increasing the pinhole diameter P, the lateral resolution of the interferometric setup increases asymptotically up to a maximum value. Furthermore, with a growing diameter of the pinhole the axial resolution decreases and disappears in case of an infinite pinhole [3]. Then the detected signal of an object point is independent of its axial position. This makes the image inversion technique suitable for the combination with established extended focus methods.

The full correlation between the pinhole diameter and the resolution has not been investigated in detail so far. Additionally, the influence on the signal-to-noise ratio (SNR) of such systems has only been considered in special cases [3,11]. So, one aim of this paper is to give a detailed view on these topics. We also investigate the impact of the pinhole size on the lateral and axial resolution, the optical transfer function (OTF) and the noise characteristics of different types of interferometrically enhanced microscopes.

2. Principles of image inversion microscopy

In image inversion microscopy, the object plane is imaged to one or two detectors after passing a two-beam interferometer.

* Corresponding author.
E-mail address: Daniel.Weigel@uni-jena.de (D. Weigel).

http://dx.doi.org/10.1016/j.optcom.2014.07.033
0030-4018/

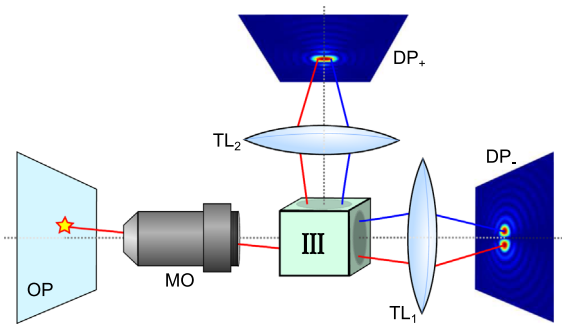

Fig. 1. Sketch of a microscope with an additional image inversion interferometer. A point source in the object plane (OP) is imaged into the detection planes ($DP_{\pm}$) through the image inversion interferometer (III). The III is placed into the parallel light beam between the microscope objective (MO) and the tube lens ($TL_{1/2}$).

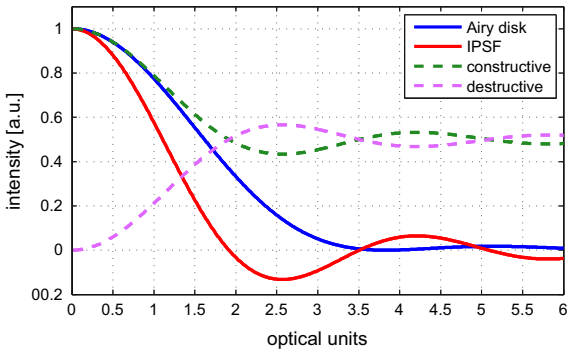

Fig. 2. Cross-section through the PSF, the IPSF and the signals at the constructive and the destructive exit of the interferometer in lateral direction. Using an open pinhole and the scalar approximation, the interferometric full width half maximum (FWHM) is about 32% smaller than the FWHM of the Airy disk.

An optical system is integrated in the interferometer creating two images in the detection plane that are spatially inverted to each other. Various types of image inversion interferometers have already been mentioned [3,6,5,11] differing only in technical details. For this reason Fig. 1 illustrates the basic setup with the help of a black-box.

A point source in the object plane is imaged into the detector plane by a microscope objective and a tube lens. So, an object point positioned at $\vec{r}_0 = (x_0,\ y_0)$ gives two images of this point at $\vec{r}_0'$ and $-\vec{r}_0'$ in the detection plane. Here, $\vec{r}_0' = -M \cdot \vec{r}_0$ is the location of the geometrical optical image with M being the associated magnification of the imaging system. Due to the fact that they have the same source, these point images are coherent to each other. The resulting intensity distribution is given by the following equation:

$$I(\vec{r}', \vec{r}_0')_{\pm} = |h(\vec{r}' + \vec{r}_0')|^2 + |h(\vec{r}' - \vec{r}_0')|^2 \pm 2 \cdot h(\vec{r}' + \vec{r}_0') \cdot h(\vec{r}' - \vec{r}_0') \quad (1)$$

The amplitude point spread function (APSF) of the imaging system is denoted by h. The first two terms in Eq. (1) represent the two point images, with the third term denoting the interference of those. The constructive exit of the interferometer is labeled by "+" and the destructive one by "−":

$$S_{\pm}(\vec{r}_0') = \int_P I(\vec{r}', \vec{r}_0')_{\pm}\, d\vec{r}' \quad (2)$$

$$\mathrm{IPSF}(\vec{r}_0') = 4 \int_P h(\vec{r}' + \vec{r}_0') \cdot h(\vec{r}' - \vec{r}_0')\, d\vec{r}'. \quad (3)$$

The integration of these intensity distributions results in the signals S_+ and S_- (Eq. (2)). Then, subtracting the signal of the destructive exit from the signal of the constructive exit suppresses the incoherent background signal. Hence, the difference gives only the integral of the interference term (Eq. (3)). The limitation of the integration area P could be realized by pinholes in front of the detectors. If the detector is spatially resolving, the integration has to be done numerically around the inversion axis. The integral is independent of the image space coordinate $\vec{r}'$, but it still depends on the position of the source point $\vec{r}_0'$. Therefore, it describes the transfer of a point through the full system consisting of imaging optics, interferometer and detectors. For this reason, it can be interpreted as an interferometric point spread function (IPSF). If the object is created by several light-emitting point sources that are incoherent to each other (e.g. fluorophores), the interferometrically improved image can be regarded as a convolution of the object distribution with the IPSF.

In scalar approximation used for low numerical apertures, the APSF is equivalent to a BSinc-function (Eq. (4), J_1 donates the Bessel function of the first kind) [12], so that the PSF of the conventional incoherent imaging system is represented by the Airy disk (Eq. (5)). Under this condition and after integrating over the full detection plane (infinite pinhole), the IPSF becomes a BSinc-function. But, in contrast to the APSF, the IPSF is a function of the doubled argument (Eq. (6)) [1,3,7]:

$$h(v) = 2\frac{J_1(v)}{v} \quad (4)$$

$$\mathrm{PSF}(v) = |h(v)|^2 = 2\left|\frac{J_1(v)}{v}\right|^2 \quad (5)$$

$$\mathrm{IPSF}(v) = 2\frac{J_1(2v)}{2v} \quad (6)$$

Factor 2 generates a narrower function compared to the incoherent PSF, as can be seen in Fig. 2, and results in an improved lateral resolution. For reasons of clarity, normalized lateral optical coordinates $v = (2\pi \cdot \mathrm{NA}/\lambda)|\vec{r}_0'|$ and the corresponding dimensionless optical units (o.u.) are used, with $\mathrm{NA} = n \cdot \sin(\alpha)$ symbolizing the numerical aperture while α denotes the half aperture angle of the microscope objective. The refractive index of the immersion fluid is n and the wavelength λ.

3. Detection PSF

Simulations with MATLAB (The MathWorks, MA, USA) have been done to investigate the pinhole's influence on the IPSF. Using vector diffraction theory for high numerical apertures [13], we simulated circular polarized illumination and unpolarized fluorescent light (detection) at $\mathrm{NA} = 1.2$ ($n = 1.33$) each. Besides the lateral optical coordinate v, the normalized axial optical coordinate $u = 2\pi \cdot z \cdot \mathrm{NA}^2/n \cdot \lambda$ and the corresponding dimensionless optical units will be used below, while z is the axial spatial coordinate.

At first, the IPSF is investigated and compared with the detection PSF of a conventional confocal microscope $\mathrm{CPSF}_{\mathrm{det}}$. According to [14] the $\mathrm{CPSF}_{\mathrm{det}}$ can be described by Eq. (7). The symbol $\otimes$ denotes a convolution:

$$\mathrm{CPSF}_{\mathrm{det}}(u, v) = P(u, v) \otimes \mathrm{PSF}(u, v). \quad (7)$$

The IPSF can be gained using the differences of the signals from the constructive and the destructive exit of the interferometer (Eq. (2)) as mentioned above. An interference peak is located on the inversion axis of the constructive signal. This peak is already smaller than the PSF of the corresponding conventional system. But due to the incoherent background intensity, it leads to a reduced contrast in the image of the constructive exit. The lateral size of this background approximately has the size of the used pinhole. As an example, the